

Raman, X-Ray Diffraction and Differential Scanning Calorimetry Studies of the Melt-Induced Changes in Uncompatibilized and Compatibilized Blends of High-Density Polyethylene and Nylon 12

Harumi Sato¹, Yukiteru Katsumoto¹, Shigehiro Sasao², Kimihiro Matsukawa², Yasuo Kita², Heinz W. Siesler³ and Yukihiro Ozaki^{1*}

¹ School of Science, Kwansei Gakuin University, Gakuen, Sanda, Hyogo 669-1337, Japan

² Plastics Department, Osaka Municipal Technical Research Institute, Morinomiya, Joto-ku, Osaka 536-8553, Japan

³ Department of Physical Chemistry, University of Essen, D45117, Essen, Germany

Summary: The crystallinity of non-molten and pre-molten uncompatibilized and compatibilized polymer blends of high density polyethylene (HDPE)/Nylon 12 have been investigated by using FT-Raman spectroscopy, differential scanning calorimetry (DSC), and wide angle X-ray diffraction (WAXD). The FT-Raman, DSC, and WAXD measurements have revealed that the crystallinity of HDPE of both uncompatibilized and compatibilized blends increases upon melting except for the compatibilized blend with the Nylon 12 content of 80 wt%. The degree of the increase is significantly larger for the uncompatibilized blends than the compatibilized blends. The FT-Raman data suggests that the crystallinity of the compatibilized blend with the Nylon 12 content of 80 wt% decreases slightly after melting. It is very likely that the compatibilized polymer blends are well oriented during the melting and molding process by an extruder because of the existence of maleic anhydride (MAH)-grafted copolymer as a compatibilizer. In contrast, it seems that the uncompatibilized polymer blends are not so much oriented and have more amorphous phase in the Nylon 12 rich region before melting. Thus, the melting process induces a recrystallization process.

Introduction

Polymer blends such as the combination of Nylon and polyethylene (PE), polypropylene (PP), or polystyrene (PS) have been matters of keen interest because they show a high notched Izot impact strength [1-7]. Nylon/PE, Nylon/PP or Nylon/PS do

not give good dispersion, if they are only mechanically blended. However, they show clear dispersion when they are blended with a maleic anhydride (MAH)-grafted copolymer as a compatibilizer [1-7]. It is very likely that a certain graft polymer is formed between MAH and HDPE, PP, or PS, providing the good dispersion.

Infrared and Raman spectroscopy have been used extensively to study the structure, orientation, and crystallinity of polymer blends and their component polymers [8-11]. It is well known that several infrared and Raman bands are very sensitive to the conformation and/or crystallinity of polymers [8-11]. We have been investigating differences in the structure and physical properties between the uncompatibilized and compatibilized polymer blends of high density polyethylene and Nylon12 (HDPE/Nylon12) by use of FT-Raman, together with wide angle X-ray diffraction (WAXD), differential scanning calorimetry (DSC) and scanning electron microscope (SEM) [12]. SEM images showed quite different miscibility between the uncompatibilized and compatibilized polymer blends. It was found from the Raman measurements that in contrast to the general trend of crystallinity of HDPE in polymer blends, the crystallinity of HDPE in the compatibilized blends becomes higher than that of HDPE in uncompatibilized blends when the Nylon 12 content increases beyond 70 wt% [12].

The purpose of this paper is to report the melt-induced changes in molecular structure, crystallinity, and physical properties in uncompatibilized and compatibilized polymer blends of HDPE/Nylon 12 investigated by using FT-Raman, WAXD, and DSC. The polymer material is subjected to an elongational stress during the preparation of pellets by an extruder. It is very important to compare the effects of the extrusion on the crystallinity between the non-molten and pre-molten polymer blends [13-17]. It is also of interest to investigate the comparison between the recrystallization by melting and the crystallization by elongation. It is known that the mechanical properties of polymer blends are closely related to their composition, phase structure and molecular orientation. The crystallinity of the blends is strongly influenced by the molecular orientation induced by stretching [18]. In the present communication we explore the influence of the melting on the crystallinity of the HDPE/Nylon 12 blends.

Experimental Section

Preparation of the Uncompatibilized and Compatibilized Blends. The HDPE used was supplied by SUNTEC-HD J240 Polyethylene (Asahi Chemical Industry Co., Ltd.) and Nylon 12 was obtained from UBE INDUSTRIES LTD. The uncompatibilized and compatibilized blends were prepared by compounding Nylon 12 with HDPE and MAH-HDPE at 220 °C in a twin-screw extruder, respectively. MAH-HDPE was prepared by use of the same extruder by supplying HDPE with MAH at 220 °C (Fig. 1).

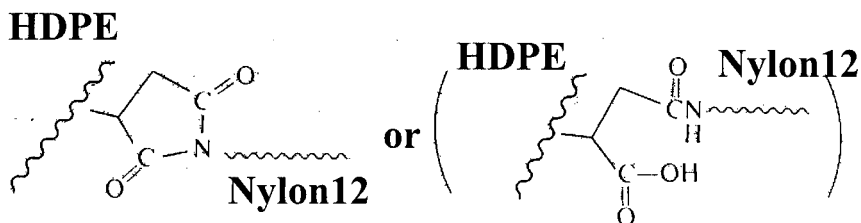


Fig. 1 The scheme of reactive HDPE/Nylon12 compatibilized polymer blends.

The concentration of MAH was adjusted to yield MAH-HDPE having 0.5wt% of MAH. Blending ratios of HDPE/Nylon 12 were 20/80, 30/70, and 50/50. Pre-molten polymer blends of HDPE/Nylon 12 were prepared by melting the polymer blends on a hotplate at about 200 °C and allowing to cool down before characterization by the different techniques.

X-ray Diffraction. The X-ray diffraction data of the HDPE/Nylon12 blends were measured at room temperature by use of a RIGAKU R-AXIS IV imaging plate diffractometer. CuK α radiation (wavelength, 1.5418 nm) was used as an incident X-ray source (40kV, 100mA).

Fourier-Transform Raman Spectroscopy (FT-Raman). The FT-Raman spectra of the HDPE/Nylon 12 blends were measured with a JEOL JRS-FT6500N FT-Raman spectrometer equipped with a cooled InGaAs detector. An excitation wavelength at 1064 nm was provided by a cw Nd:YAG laser (Spectron SL301), and the laser power at

the sample position was typically 200 mW. Raman scattered light was collected in a 180° back scattering geometry. The Raman data were obtained at a spectral resolution of 4 cm^{-1} and 500-1000 scans were coadded to ensure a high signal-to-noise ratio.

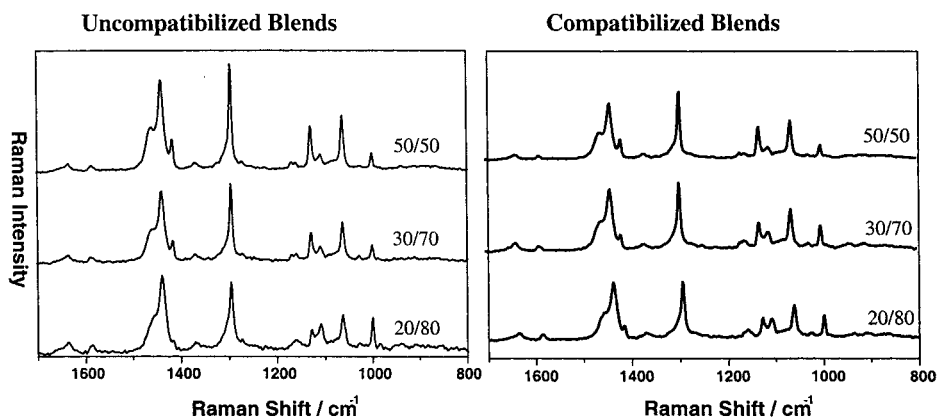
Differential Scanning Calorimetry (DSC). DSC measurements were performed on a SEIKO EXSTAR6000 with a DSC6200 module apparatus over a temperature range from -140 to 230°C at heating and cooling rates of 10°Cmin^{-1} .

Results and Discussion

Figure 2 shows FT-Raman spectra of (a) non-molten and (b) pre-molten uncompatibilized and compatibilized polymer blends of different composition (20/80, 30/70, and 50/50). It can be clearly seen that the intensity ratio of the two bands at 1129 and 1110 cm^{-1} changes between the uncompatibilized and compatibilized polymer blends and between the non-molten and pre-molten blends of HDPE/Nylon 12. Furthermore, Raman bands of the pre-molten polymer blends are more intense and sharper than those of the non-molten polymer blends. This is because the polymer blends are recrystallized and reoriented partially during the melting process. The assignments of the Raman bands of HDPE/Nylon 12 polymer blends are shown in Table I [12, 19-21].

The bands at 1129 and 1110 cm^{-1} are due to symmetric C-C stretching vibrations of all-trans alkyl chains of $\text{CH}_3(\text{CH}_2)_n\text{CH}_3$ for $n>6$ and C-C stretching vibrations of alkyl chains of Nylon 12, respectively [8-10]. Therefore, one can discuss the degree of crystallinity of HDPE by using the intensity ratio of two bands at 1129 and 1110 cm^{-1} (I_{1110}/I_{1129}) [12]. We used the band at 1110 cm^{-1} as an internal standard. This internal standard is valid when we compare crystallinity of HDPE in the blends having the same blend ratio. In our previous study it was found that for the non-molten polymer blends, the intensity ratio is higher for the compatibilized blend ($I_{1110}/I_{1129}=0.63$) than for the uncompatibilized one (0.48) when the Nylon 12 content is 70wt% while for the blends with the Nylon 12 content of 80wt% the intensity ratio is reversed [12] (Fig. 2(a)).

(a) Non-Molten Polymer Blends



(b) Pre-Molten Polymer Blends

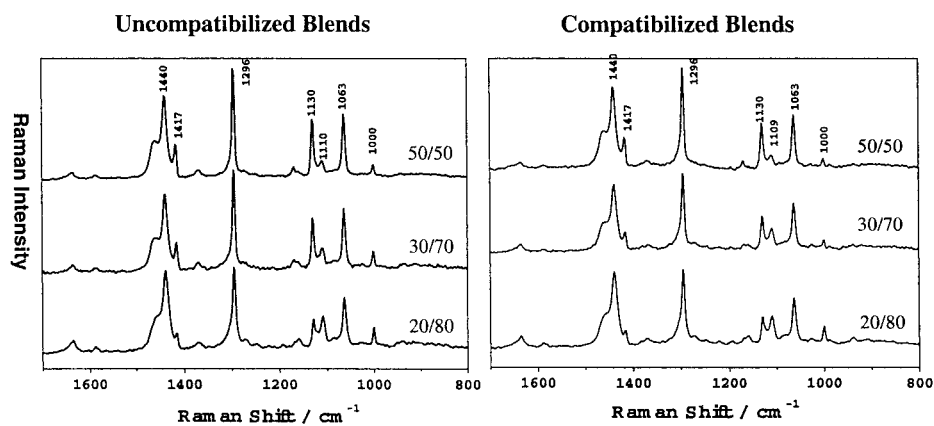


Fig. 2 FT-Raman spectra of HDPE/Nylon 12 blends; (a) non-molten blends, (b) pre-molten blends.

Similar result are obtained for the pre-molten blends as shown in Figure 2(b). However, it should be noted that the difference in the ratio is much smaller for the pre-molten uncompatibilized and compatibilized polymer blends than for the non-molten polymer blends with the Nylon 12 content of 80 wt% (Figure 2). The composition of Figure 2(a) and (b) suggests that the crystallinity of uncompatibilized blends becomes higher upon melting while that of compatibilized blends becomes higher a little for a Nylon 12 content of 70wt% and lower for a Nylon 12 content of 80 wt%.

The Raman spectra in Figure 2 show other evidences for the increase in the crystallinity of the uncompatibilized polymer blends with Nylon 12 contents of 50, 70, and 80wt%. For example, the relative intensities of the bands at 1439, 1418, and 1063 cm^{-1} which are characteristic of the crystalline phase become stronger after melting (Figure 2 (b)). It seems that the compatibilized polymer blends are already oriented by the extruder during the melting and molding process due to Nylon 12 grafted with MAH-HDPE, while the uncompatibilized polymer blends, which are not so much oriented, have more amorphous parts in the Nylon 12 rich regions before melting. Therefore, the uncompatibilized polymer blends are more easily subjected to the melt-induced recrystallization.

Table I Assignments of the Raman Bands of HDPE/Nylon 12

Frequency / cm^{-1}		Assignments	Features
Nylon12	HDPE		
1063	1063	asymmetric C-C stretching	all-trans $-(\text{CH}_2)_n$
1110		symmetric C-C stretching	
	1129	symmetric C-C stretching	all-trans $-(\text{CH}_2)_n$
1296	1296	CH_2 twisting	all-trans $-(\text{CH}_2)_n$
	1418	CH_2 bending	crystalline
1440	1440	CH_2 bending	crystalline
1636		amide I	

Figure 3 (a) and (b) show the WAXD patterns of the non-molten and pre-molten uncompatibilized polymer blend of HDPE/Nylon 12 (30/70). The half-width of the PE(110) reflection of the pre-molten uncompatibilized polymer blend is sharper than that of the non-molten blend, indicating that the crystallinity increases upon melting. Similar results were obtained also for the uncompatibilized blends with the Nylon content of 50 and 20 wt%.

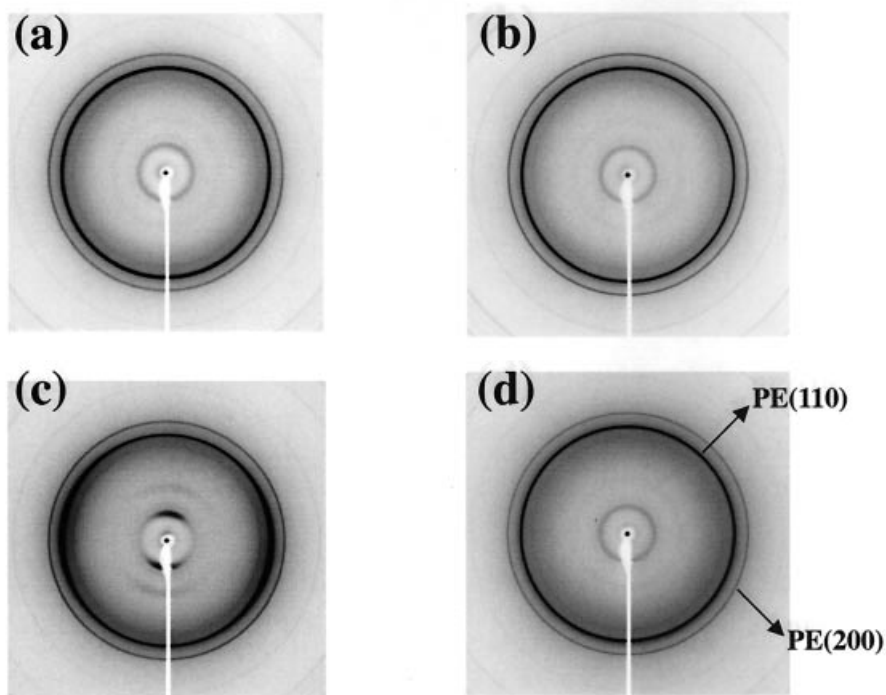


Fig. 3 Wide-angle X-ray diffraction patterns of (a) uncompatibilized polymer blend (30/70), (b) pre-molten uncompatibilized polymer blend (30/70), (c) compatibilized polymer blend (30/70) and (d) pre-molten compatibilized polymer blend (30/70).

Figure 3 (c) and (d) compare the WAXD patterns of the non-molten and pre-molten compatibilized polymer blend of HDPE/Nylon 12 (30/70). Note that there is a clear difference in the X-ray diffraction pattern between the non-molten and pre-molten polymer blend; the non-molten polymer blend shows an anisotropic structure pattern, whereas the pre-molten polymer blend does not show such a pattern. The compatibilized HDPE/Nylon 12 (50/50 and 20/80) yield similar results to that of HDPE/Nylon 12 (30/70). The anisotropic structure is specific for the compatibilized polymer blend. It can be seen from Figure 3(c) and (d) that the elongational stress of the compatibilized polymer blend disappears during the melting process. It is rather difficult to discuss the crystallinity from the X-ray diffraction patterns of compatibilized blends because one cannot estimate the half-width of the PE(110) reflection for the non-molten blends due to the anisotropy pattern.

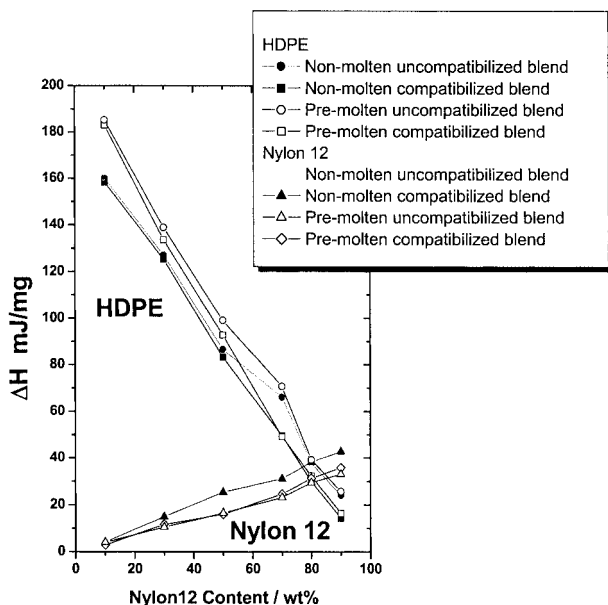


Fig. 4 Dependence of the heats of fusion of HDPE and Nylon 12 on the Nylon 12 content for the non-molten and pre-molten uncompatibilized and compatibilized polymer blends of HDPE/Nylon 12.

Figure 4 presents the heats of fusion derived from DSC thermograms of the non-molten and pre-molten uncompatibilized and compatibilized polymer blends with the Nylon 12 content varying from 10 to 90 wt%. No significant difference is observed between the first heating and the second heating. The ΔH of HDPE of the pre-molten polymer blends are larger than those of the non-molten blends, while the ΔH of Nylon 12 of the pre-molten polymer blends are smaller than that of the non-molten blends. Consequently, the results suggest that the crystallinity of the HDPE increases while that of Nylon 12 decreases upon melting.

Conclusion

The melt-induced changes in the crystallinity of uncompatibilized and compatibilized polymer blends of HDPE/Nylon 12 have been investigated by the Raman spectroscopy, WAXD, and DSC measurements. The intensity and sharpness of the Raman bands of the uncompatibilized and compatibilized polymer blends vary upon melting. The intensity ratio of the two bands at 1129 and 1110 cm^{-1} has revealed that the crystallinity of the uncompatibilized polymer blends increases more significantly than that of the compatibilized ones after melting. In the case of the compatibilized blend with the Nylon 12 content of 80wt%, the crystallinity decreases during the melting process.

The non-molten and pre-molten compatibilized polymer blends have shown quite different reflection patterns by WAXD. The anisotropy pattern, characteristic of compatibilized blends, disappears upon melting. The half-width of the X-ray diffraction reflections of the pre-molten uncompatibilized polymer blends is significantly narrower than that of the non-molten polymer blend, suggesting that the crystallinity of the uncompatibilized polymer blends increases during the melting process.

The DSC measurements have shown that the ΔH of HDPE of the pre-molten polymer blends is larger than that of the non-molten blends. This suggests that the crystallinity of HDPE of the polymer blends increases during the melting process.

Acknowledgments

The authors would like to thank Dr. Hiroshi Yamaguchi (Kwansei-Gakuin University) for assisting with the WAXD measurements.

References

1. F. Ide and A. Hasegawa, *J. Appl. Polym. Sci.*, **18**, 963(1974).
2. C. C. Chen, E. Fontan, K. Min, and J. L. White, *Polym. Eng. Sci.*, **28**, 69(1988).
3. S. Y. Hobbs, R. C. Bopp, and V. H. Watkins, *Polym. Eng. Sci.*, **23**, 380(1983).
4. L. A. Utracky, M. M. Dumoulin, and P. Toma, *Polym. Eng. Sci.*, **26**, 34(1986).
5. D. Heikens and W. Barensten, *Polymer*, **18**, 69(1977).
6. D. Heikens, N. Hoen, W. Barensten, P. Piet and H. Ladan, *J. Polym. Sci. Symp.*, **62**, 309(1978).
7. W. M. Barensten, D. Heikens and P. Piet, *Polymer*, **15**, 119(1974).
8. P. A. Bentley, P. J. Hendra, *Spectrochim. Acta*, Part A, **51**, 2125 (1995).
9. M. Glotin, R. Domszy, L. Mandelkern, *J. Polym. Sci.: Polym. Phys. Ed.* **21**, 285 (1983).
10. A. Tarazona, E. Koglin, B. B. Coussens, R. J. Meier, *Vib. Spectrosc.* **14**, 159(1997).
11. G. R. Strobl and W. Hagedorn, *J. Polym. Sci. Polym. Phys. Ed.* **16**, 1181(1978).
12. H. Sato, S. Sasao, K. Matsukawa, Y. Kita, H. Yamaguchi, H. W. Siesler, and Y. Ozaki, submitted.
13. J. Kratochvil, A. Sikora, J. Baldrian, J. Dybal, R. Puffr, *Polymer*, **41**, 7653(2000).
14. J. Kratochvil, A. Sikora, J. Baldrian, J. Dybal, R. Puffr, *Polymer*, **41**, 7667(2000).
15. XL Ji, WJ Zhang, ZW Wu, *J. Polym. Sci. B: Polym. Phys.* **35**, 431(1997).
16. Petrillo E, Russo R, D'Anielli C, Vittoria V., *J. Macromol. Sci. Phys.* **B37**, 15(1998).
17. P. Schmidt, J. Baldrian, J. Scudla, J. Dybal, M. Raab, K.-J. Eichhorn, *Polymer*, **42**, 5321(2001).
18. P. Schmidt, J. Kolarik, F. Lednický, J. Dybal, J.M. Lagaron, J.M. Pastor, *Polymer*, **41**, 4267(2000).
19. Y. Ren, M. Shimoyama, T. Ninomiya, K. Matsukawa, H. Inoue, I. Noda, and Y. Ozaki, *J. Phys. Chem. B*, **103**, 6475(1999).
20. P. J. Hendra, W. F. Maddams, I. A. Royaud, H. A. Willis, and V. Zichy, *Spectrochim. Acta* **46A**, 747(1990).
21. J. K. Agbenyega, G. Ellis, P. J. Hendra, W. F. Maddams, C. Passingham, H.A. Willis, and J. Chalmers, *Spectrochim. Acta* **46A**, 197(1990).